2015

Normalizing Tumor Vasculature Using Sepiapterin to Increase Radiosensitivity

Ninu Bruno

Normalizing Tumor Vasculature Using Sepiapterin to Increase Radiosensitivity

A thesis submitted in partial fulfillment of the requirements for the degree of Master of Science at Virginia Commonwealth University.

by

Ninu Bruno

Bachelor of Science, Texas A&M University, 2013

Ross B. Mikkelsen, PhD

Professor and Division Chair, Department of Radiation Oncology

Virginia Commonwealth University

Richmond, VA

November 18, 2015

TABLE OF CONTENTS

ABSTRACT

NORMALIZING TUMOR VASCULATURE USING SEPIAPTERIN TO INCREASE RADIOSENSITIVITY

By Ninu Bruno, B.S.

A thesis submitted in partial fulfillment of the requirements for the degree of Master of Science at Virginia Commonwealth University.

Virginia Commonwealth University, 2015

Advisor: Ross B. Mikkelsen, PhD

Professor and Division Chair, Department of Radiation Oncology

Our studies examine the role of nitric oxide synthase (NOS) in tumor vasculature. NOS is “uncoupled” in tumor cells, resulting in peroxynitrite ($ONOO^-$) formation in lieu of nitric oxide (NO). NO signaling is critical for vascular function, thus uncoupling of eNOS in endothelial cells may partly explain the poor vasculature found within tumors. NOS can be “recoupled” through Sepiapterin (SP) treatment of tumor cells. We examined whether SP could normalize tumor vasculature, promoting radiosensitivity. Optoacoustic

tomography of flank xenografts and spontaneous tumor models demonstrate that SP significantly enhances percent oxyhemoglobin in tumors. Immunohistochemical analysis of SP-treated tumors showed significant reduction in CD31 staining and significant increases in smooth muscle actin (SMA), both hallmarks of vascular normalization. SP resulted in over a two-fold increase in apoptosis with irradiation. These data demonstrate potential for SP as an adjuvant in cancer treatment. Future studies will examine drug uptake and mechanisms behind vascular normalization.

INTRODUCTION

Tumor Vasculature

Unlike the vessels in normal tissues, the vasculature in tumors is abnormal [1]. Normal vessels are highly organized, evenly distributed, and well-differentiated. In contrast tumor vessels are convoluted, chaotic, and irregular [2]. Tumor vessels are not only structurally abnormal, but are functionally abnormal as well. The basement membrane of tumor vessels tends to be unusually thick or thin and have loosely attached pericytes, or vascular smooth muscle cells. The endothelial cells of the basement membrane are also sporadically dispersed throughout these vessels [1]. The aberrant nature of the vasculature results in uneven, heterogeneous blood flow and leaky, hemorrhagic blood vessels. The leakiness of the vessels increases interstitial fluid pressure and may lead to swelling. When tumor cells have outgrown their blood supply, pockets of hypoxia can develop due to poor perfusion, promoting tumor metastasis and progression [3]. Poor perfusion also limits the access and efficient delivery of therapeutic drugs.

While neovascularization refers to the formation of completely new blood vessels, the development of blood vessels from existing vasculature is known as angiogenesis [4]. An expanded vasculature can increase the nutrient and oxygen supply to tumors [1]. Angiogenesis is therefore vital for the growth, invasion, and metastasis of tumors [5, 6, 7]. In tumors the balance between proangiogenic and antiangiogenic pathways is disrupted, favoring angiogenesis.

Angiogenic switch is the initiation of angiogenesis by a previously dormant tumor. The switch is typically triggered by hypoxia or nutrient deprivation, causing the tumor to secrete cytokines and growth factors that induce the migration of endothelial cells towards the tumor mass [8]. The endothelial cells form hollow tubes that eventually become a network of mature blood vessels. Hypoxia within the inner mass of the tumor promotes the nuclear translocation of hypoxia-inducible factor 1 (HIF-1). This subsequently activates numerous proangiogenic genes, including vascular endothelial growth factor (VEGF) [9].

The binding of VEGF to its receptor leads to angiogenesis by mediating proliferation, vascular permeability, cell migration, and cell survival [9]. VEGF can signal via the mitogen-activated protein kinase/ extracellular signal-regulated kinase (MAP/ERK) pathway to activate gene expression and cause cell proliferation. VEGF activates phospholipase C-γ by producing diacylglycerol and inositol triphosphate (IP3), raising intracellular Ca^{2+} concentration [10]. Endothelial NOS is activated and generates NO due to increased intracellular Ca^{2+}. Increased intracellular Ca^{2+} also activates cytosolic phospholipase A and prostaglandin production. Production of NO and prostaglandins induces vascular permeability [9].

Stimulation of VEGF signaling has also been demonstrated to upregulate focal adhesion kinase [11]. The activation of this pathway leads to focal adhesion turnover and cell migration. Heat shock protein 27 is induced by VEGF signaling through p38 and results in actin reorganization and cell migration [12, 13]. VEGF activation of phosphoinositide-3-kinase (PI3K) converts phosphatidylinositol (4, 5)-bisphosphate to phosphatidylinositol (3, 4, 5)-triphosphate (PIP_3) [9]. Akt is then recruited to the cell

membrane by PIP_3 and is phosphorylated. Akt can not only activate NOS, but also inhibit proapoptotic proteins caspase 9 and Bcl-2 associated death promoter (BAD) [14]. Inhibition of these proteins leads to cell survival [15].

Matrix metalloproteinases (MMPs), which are also induced by HIF-1, break down the extracellular matrix to aid endothelial cell migration and the release of associated growth factors [9]. Tumor-associated macrophages (TAMs) are activated by factors secreted into the tumor microenvironment. TAMS produce VEGF, MMPS, and other angiogenic factors [16]. During tumor angiogenesis endothelial cells recruit pericytes for structural support promoting tumor survival [17]. Endothelial cells secrete platelet-derived growth factor (PDGF) which binds to its receptor on the pericyte membrane. The binding of PDGF to PDGF receptors results in the production and secretion of VEGF by pericytes. VEGF then signals through the endothelial VEGF receptor, further promoting angiogenesis [16]. Initiation of blood vessel growth not only requires up-regulation of angiogenic factors, but down-regulation of antiangiogenic factors as well.

Angiogenesis can be detected by measuring CD31, a platelet-endothelial adhesion molecule, as an endothelial cell marker. Hvingel showed that CD31 staining intensity is significantly stronger in cancer microvessels compared to benign endometrial polyp microvessels [18]. While CD31 is a useful molecular marker for endothelial cells, α-smooth muscle actin (α-SMA) is commonly used to identify pericytes. One of six isoforms of actin, α-SMA is typically reserved to cells derived from smooth muscle lineages. Tonino and Abreu showed that α-SMA expression is greater in the periphery of gastrointestinal cancer cells than in the center and metastatic regions, suggesting the blood vessels in these regions are delicate and immature [19].

The Role of Nitric Oxide in Tumor Vasculature

Nitric oxide (NO) is crucial in vasoregulation, signaling within the central nervous system, and immune responses [20]. Under normal, physiologic conditions nitric oxide synthases (NOS) produce nitric oxide [21]. There are three isoforms of NOS: nNOS (NOSI), iNOS (NOSII), and eNOS (NOSIII) [22]. Depending on the tumor type, tumor cells may express one or multiple isoforms [23]. With tetrahydrobiopterin (BH4) as a cofactor, NOS transfers electrons from its reductase domain to its oxidase domain. The electrons are then used to oxidize L-arginine to produce NO and L-citrulline in the presence of oxygen. NO has a dual role in cancer, and exhibits both pro- and anti-tumor effects [23].

NO can either promote or inhibit angiogenesis. The ultimate effect of NO depends on NO concentration, duration of exposure, activity, distribution, and cell sensitivity to NO. NO mediates numerous angiogenic effectors through complex mechanisms and various pathways. Growth factors, cytokines, metabolic stress, and shear stress stimulate the release of NO by upregulating NOS. NO activates multiple signaling pathways through *S*-nitrosylation and cyclic guanosine monophosphate (cGMP). NO can form *S*-nitrosothiols through three different pathways: a direct reaction, auto-oxidation of NO, or catalysis at metal centers and these nitrosothiols are important determinants of cell fate. *S*-nitrosylation of the cysteine in position 163 of caspase 3 inhibits its activity. When cysteine-188 of p21Ras is *S*-nitrosylated, however, its activity is stimulated. Caspase 3 inhibition causes decreased apoptosis and Ras activation causes increased proliferation and migration of endothelial cells. NO also increases

endothelial cell proliferation and migration by activating protein kinase Cα (PKCα) and inhibiting PKCδ [23].

Another pathway that plays an important role in NO-mediated angiogenesis is the soluble guanylyl cyclase (sGC)–cGMP pathway. NO induces a conformational change in sGC by binding to the sixth coordinating position of its heme iron. Binding results in a 200-fold activation of the enzyme and enhanced synthesis of cGMP from guanosine triphosphate (GTP) [24]. cGMP then activates the MAPK/ERK pathway by upregulating Ras and cGMP-dependent protein kinase (PKG), which interacts with Raf. Ultimately, the DNA binding activity of activator protein 1 (AP1) is increased, resulting in increased cell proliferation and migration. PKG appears to mediate cell migration by producing matrix metalloproteinase 13 (MMP13) via ERK and by Akt activation through PI3K [25].

Human and experimental tumors provide a positive correlation between NO and tumor progression. The degree of malignancy for tumors of the central nervous system, reproductive tract, and breast have been shown to be related to NOS protein concentration and activity. The idea that NO plays a direct role in tumor growth and metastasis is supported by experimental tumor models [26, 27]. Tumor growth and vascularity in nude mice was stimulated by upregulation of NOS in a human colonic adenocarcinoma cell line. This effect can be blocked by a selective inhibitor, 1400W [26]. In ovarian cancer studies, exogenous NO increased VEGF and angiogenesis. When inhibited with NG-nitro-L-arginine methyl ester (L-NAME), VEGF expression in the ovarian cell lines was significantly reduced and angiogenesis was inhibited [27].

Studies on endogenous inhibitors of NOS, including asymmetric dimethyl arginine, further suggest that tumor growth and angiogenesis is associated with the

increased availability of NO [28]. Despite evidence implicating NO as an inducer of tumor progression, reports suggest that it may also inhibit progression. Elevated NO levels have a cytotoxic effect on tumor cells. Endogenous NO has also been shown to induce apoptosis in pancreatic, breast, and colon cancer [23].

Tumor Vasculature and Therapeutic Efficacy

Jain proposed that restoring the balance between pro- and anti-angiogenic pathways would remodel tumor vasculature and normalize it, increasing perfusion and oxygenation of tumors [1]. Anti-angiogenic treatment generally involves either intracellular inhibition of receptor tyrosine kinases, or inhibition of angiogenic factors and their receptors. Bevacizumab, a VEGF inhibitor, was approved for breast cancer treatment and management of advanced colon cancer in 2004 [4]. Tumor blood vessels have also been shown to be normalized by reestablishing NO gradients around vessels in human glioma cells. Kashiwagi showed that elimination of nonvascular NO production and establishment of the perivascular NO gradient alters the morphology and function of tumor vasculature and increases oxygenation [29].

One drawback of normalization using antiangiogenic therapy is that the improved blood supply may also lead to more efficient delivery of nutrients to the tumor cells [30]. The benefits of anti-angiogenic therapy also appear to be transient in preclinical and clinical settings [31]. In recent years, there has been debate over whether a pro-angiogenic or anti-angiogenic approach is more effective for tumor treatment [32]. A novel strategy known as “vascular promotion therapy” has been proposed to treat tumors by stimulating, rather than preventing, vascular formation [33].

A factor that limits the effectiveness of radiation therapy in various cancers is radioresistance [34]. The hypoxic nature of tumors helps contribute to radioresistance [22]. The damage caused by free radicals in the DNA as a result of radiation can be repaired under hypoxic conditions, but cannot be repaired when molecular oxygen is available [35]. Oxygen acts as a source of free radicals which can further damage tumors. In 90% of solid tumors, the median concentration of oxygen in tissues is below the normal 40-60 mm Hg. In 50% of solid tumors, the median oxygen concentration is below 10 mm Hg [36]. When compared to normal cells, hypoxic tumors are two- to three-fold less sensitive to radiation [37].

One mechanism by which tumors grow back after radiotherapy is repopulation [38]. It has been shown that cell death by radiation is an important signal for repopulation after radiotherapy. Irradiation (IR) of tumor cells can lead to proliferation of cells that were not irradiated, both *in vivo* and *in vitro*. Activation of caspase 3 in dying cells is integral for proliferation signals [39]. Another limitation of radiotherapy is tumor stem cells. These cells can regenerate the tumor [37]. Tumor stem cells are also implicated in resistance to chemotherapeutic agents [40].

It has been suggested that NO donors may inhibit EMT, metastasis, and reverse drug resistance [41]. In one study, DETANONOate was shown to inhibit epithelial-mesenchymal transition (EMT) in metastatic human prostate cells. NO donors, like DETANONOate, mimic endogenous NO production [42]. Gao demonstrated that DETANONOate radiosensitizes HT-29 colorectal cancer cells and xenografts. HT-29 cells and xenografts had previously been shown to be highly radioresistant [43]. In the xenograft model, human tumor cells are either subcutaneously injected or transplanted

into an organ of mice. The mice are immunocompromised and do not reject human cells [44]. Hypoxic murine mammary adenocarcinoma EMT-6 cells also showed radiosensitization with the NO donors SNAP and PAPA/NO. NOS inhibitors reversed radiosensitization, suggesting that the radiosensitizing effects are due to the production of NO [45].

In addition to NO, NOSs are also a source of reactive oxygen species (ROS) and reactive nitrogen species (RNS) [46]. Under normal physiological conditions, when there is sufficient BH4, NOS is said to be “coupled.” Under conditions of oxidative stress and chronic inflammation, BH4 is oxidized to dihydrobiopterin (BH2). Given that NOS has an equal affinity for both BH4 and BH2, when more BH2 is present than BH4, NOS is “uncoupled” and molecular oxygen is oxidized, producing superoxide and peroxynitrite [47]. Since BH4 levels are higher than BH2 levels when NOS is coupled and the reverse is true when NOS is uncoupled, the ratio of BH4 to BH2 can be used to determine whether NOS is in the coupled or uncoupled state. The BH4:BH2 ratio is high in normal tissues and low under inflammatory conditions. Our laboratory has previously shown that the BH4:BH2 ratio is lower in various cancer cells lines than in normal tissue [48]. Our laboratory has also shown that treatment of the cancer cell lines with sepiapterin, a precursor of BH4, increases the BH4:BH2 ratio [48].

In this thesis, I intend to determine the effects of sepiapterin on tumor vasculature in A549 xenograft and MMTV spontaneous tumor models. I expect sepiapterin to recouple NOS and increase NO production in the tumors. This will lead to increased perfusion and oxygenation of the tumor, resulting in radiosensitization.

Ultimately, this will allow for more efficient delivery of therapeutic drugs and better response to radiation therapy.

MATERIALS AND METHODS

Chemicals and Reagents

L-Sepiapterin (#11.225) was from Schircks Laboratories (Jona, Switzerland). Ascorbic Acid (A5960), Potassium Iodide (P-4286), Iodine (20,777-2), Trypsin (T9201), Collagenase (C0130), DNase (D4527), Goat Serum (G9023-10ML), and Hoechst 33342 (B2261-25MG) were from Sigma Aldrich. Hydrochloric Acid (A144-212), Sodium Hydroxide (SS255-1), HPLC grade Methanol (A452-4), HPLC grade Water (W5-4), HPLC grade Acetonitrile (26827-0040), Perchloric Acid (A229), and Bovine Serum Albumin (BP1600-1) were purchased from Fisher Scientific. The cGMP EIA kit (581021) was purchased from Cayman Chemical. PBS (10010-023), Dulbecco's Modified Eagle Medium Nutrient Mixture F-12 (11330-032), Penicillin Streptomycin (15240-062), Alexa Fluor® 488 Donkey anti-Rat IgG Secondary Antibody (A-21208), and Alexa Fluor® 488 Goat anti-Mouse IgG Secondary Antibody (A-11001) were purchased from Invitrogen.

Anti-Actin Antibody (CBL171) and ApopTag® Plus Fluorescein *In Situ* Apoptosis Detection Kit (S7111) were purchased from Millipore. Purified Rat Anti-Mouse CD31 Antibody (550274) was purchased from BD Biosciences and Triton X-100 (789 704) was purchased from Roche Diagnostics. M.O.M.™ Mouse IgG Blocking Reagent was purchased from Vector Laboratories as part of the Vector® M.O.M.™ Basic Immunodetection kit (BMK-2202). Nu/Nu mice were purchased from NCI.

For animal studies involving treatment with SP, stock solutions of 0.8 mg/ml in H_2O were frozen at -20˚C. When ready for use, they were thawed and 1 ml was diluted to 40ml in animal drinking H_2O. For tissue culture studies involving SP I used tissue

culture medium as the solvent to make a 1 mM stock solution which could then be diluted as necessary. This solution was made fresh each time cells were to be treated.

Cell Culture

A549 cells were from ATCC. All cell lines were grown as monolayers in Dulbecco's Modified Eagle Medium Nutrient Mixture F-12 (Ham) supplemented with 10% FBS and 50 units/ml penicillin and streptomycin. Cells were incubated at 37˚C in 5% CO_2. Cells were passaged as necessary.

Mouse Tumor Xenografts

A549 cells were trypsinized and counted. 1.5 x 10^6 cells in 50 µl PBS were injected into each flank of 8 week old Nu- / Nu- mice from NCI.

MMTV neu mice that developed spontaneous mammary tumors were provided by Dr. Jolene Windle (VCU Dept. of Human and Molecular Genetics).

BH4 and BH2 measurements

To analyze biopterin levels in tumors animals were euthanized. Once the animal was sacrificed, the tumor was harvested and snap frozen in liquid nitrogen. The tissue was either placed in the -80˚C freezer or immediately homogenized in 10 volumes of 0.1N HCl with a pestle and mortar kept on ice. The resulting tissue homogenate was centrifuged for 20 min at max speed and the supernatant would be stored in aliquots at -80˚C.

The protocol for HPLC analysis was adapted from Woolfe et al (1983). Three solutions were needed in order to perform the acid/alkaline oxidation: 2% I_2/3% KI in 0.1N HCl, 2% I_2/3% KI in 0.2N NaOH, and 2.5% Ascorbate in 0.4 N $HClO_4^-$. 100 µl of sample was incubated with 62.5 µl of the HCl solution in one tube while another 100 µl of sample was incubated with the NaOH solution for 1 h at room temperature in the dark. After 1 h, 0.5 volumes of the ascorbate solution were added to each tube and the samples were centrifuged at 12,000 RPM for 10 min. 50 µl of the resulting supernatant from each sample was separated by HPLC on a Whatman RTF partisphere column using 5% methanol as the mobile phase at a flow rate of 1.0 ml/min and fluorescent detection at 350/450 nm.

To determine the BH4:BH2 ratio, the acidic and alkaline chromatograms for each sample were compared. Under acidic conditions both BH4 and BH2 were converted to biopterin and eluted in one peak, while under alkaline conditions BH4 was converted to pterin and now eluted in a different peak. The BH4:BH2 ratio was obtained by comparing the areas under the curve.

Determination of cellular cGMP content

Some of the supernatant aliquots from the samples harvested in 0.1 N HCl for BH4:BH2 analysis were used to make these measurements. A cGMP EIA kit from Cayman Chemical was purchased and the directions were followed as described in the manual. The samples were not acetylated.

Optoacoustic Imaging

In multispectral optoacoustic tomography (MSOT), tissues are excited by multiple-wavelength illumination, and in response to light absorption, thermoelastic materials (like hemoglobin) produce ultrasonic waves. Since oxyhemoglobin absorbs light at a lower wavelength than deoxyhemoglobin, MSOT was used to compare the oxygenation of hemoglobin in SP-treated animals to control animals.

MSOT imaging was performed using an MSOT inVision 256-TF small animal scanner (iThera Medical GmbH, Munich, Germany). It is a commercially available implementation of the imaging system, featuring a 256 element transducer array. It also uses a specifically developed, proprietary laser system (InnoLas Laser GmbH, Krailling, Germany) of equal energetic characteristics and pulse width, with fast wavelength tuning in between laser pulses. It also features an integrated laser pulse energy correction that enables the correction of each laser pulse with its measured energy, inherently compensating for the laser's wavelength-dependent energy profile. The laser system provides excitation pulses with a duration of 9 ns at wavelengths from 680 nm to 980 nm at a repetition rate of 10 Hz. For defining the oxy- and deoxyhemoglobin signals, a minimum of the following wavelengths were used in all acquisitions: 700 nm, 730 nm, 760 nm, 800 nm, 860 nm, 900 nm. A light strip of about 8 mm width on the mouse is evenly illuminated from 10 arms of a fiber bundle arranged at an angle of 13 degrees to the imaging plane. The laser delivers a radiant exposure well below the maximum permissible exposure (MPE) in living subjects. In order to correct the acquired multispectral data, the laser's energy profile was measured at the wavelengths used for the acquisition of MSOT data. A cylindrically focused 256 element ultrasound

transducer array at a center frequency of 5 MHz covers an angle of 270 degrees around the sample to create cross-sectional images. The photoacoustic signals in the μV range captured by all transducer elements are digitized simultaneously using specialized acquisition electronics (Falkenstein Microsysteme GmbH, Taufkirchen, Germany) at a sampling rate of 40 megasamples/s. Mice are submerged in a water tank in a horizontal position in a holder and are wrapped in a thin polyethylene membrane to prohibit direct contact between water and mouse but still allow for acoustic coupling. Anesthesia and oxygen are supplied through a breathing mask. The mouse and holder can be translated using a linear stage (IAI Industrieroboter GmbH, Schwalbach, Germany) to enable imaging of multiple transverse slices. The resolution of the translational stage was 0.5 mm.

In order to create an image at one wavelength, signals from 20 subsequent excitation pulses were averaged in order to compensate for laser pulse fluctuations and animal motion as well as to improve signal-to-noise ratio (SNR). Images were reconstructed using a standard back-projection algorithm, and three-dimensional images were reconstructed using the interpolated model-matrix inversion. Both were applied from within the ViewMSOT software suite supplied with the iThera Medical system. After image reconstruction, linear spectral unmixing was applied to detect and separate oxy- and deoxy-hemoglobin signals from other photo-absorbing tissue elements. For each pixel in the image, the method fits the total measured optoacoustic spectrum to the known absorption spectra of oxy- and deoxy-hemoglobin and that of the agent to be detected. This produces individual component images, each visualizing the bio-distribution of the respective absorber. The oxy- and deoxy-hemoglobin signal

intensities in the tumors were calculated by drawing regions of interest (ROI) over the tumors and measuring the respective signal intensities within those ROIs. (Method from Dr. Sundaresan Gobalakrishnan, VCU Center for Molecular Imaging.)

Immunohistochemistry

For CD31 endothelial cell and smooth muscle actin staining, frozen tumors embedded in OCT were sectioned at 6 µm. Tumor sections were fixed in -20˚C acetone for 10 min at 4˚C. The sections were first washed for 5 minutes with 1X PBS before being washed with deionized water. After serum (10% goat serum, 1% bovine serum albumin, and 0.1% triton X-100 in PBS) blocking for 1 h, the sections were washed twice with 1X PBS for 3 minutes and then washed again with deionized water. For smooth muscle actin staining, the blocking serum also included 3.6% M.O.M.™ Mouse IgG Blocking Reagent.

The sections were then stained with appropriate primary antibody overnight at 4˚C, followed by three washes for 5 minutes with 1X PBS and one wash with deionized water. The sections were incubated with Alexa488-labeled secondary IgG (Invitrogen) at room temperature for 1 hour. Sections were again washed thrice for 5 minutes with 1X PBS and washed once with deionized water. For four minutes, sections were incubated with Hoechst for nuclear staining and subsequently washed one final time with deionized water. Images were captured using the Ariol Digital Pathology Platform and quantified using ImageJ.

ApopTag® Plus Fluorescein *In Situ* Apoptosis Detection Kit from Millipore was purchased and used to detection apoptotic cells in the frozen sections.

Ex-vivo Clonogenic Cell Survival Assay

Tumors were harvested and minced into small pieces with a scalpel in medium without serum. The pieces were washed twice in medium and then the pieces were agitated in medium containing 0.08% collagenase and 0.5% Trypsin for 40 min at 37˚C. DNase to 0.06% was added to the medium and the cells were strained through a 0.70 µM cell strainer. The resulting single cell suspension was counted, excluding RBC's, and plated at different concentrations. The plating efficiency of this type of experiment is very poor so more cells were plated than I plated for the tissue culture assay. I plated 500 and 1k cells per 100 mm dish. The dishes were fixed in -20ºC methanol, stained with 0.5% crystal violet, and counted when colonies reached approximately 100 cells.

RESULTS

SP increases the BH4:BH2 ratio in A549 xenograft tumors.

The BH4:BH2 ratio was determined using xenograft tumors from athymic nude mice that were treated with 1 mg/kg/ml SP daily for six days via drinking water. Our lab has previously shown that SP treatment increases the BH4:BH2 ratio in various cancer cell lines. To determine if this held true for the A549 cell line, the BH4:BH2 ratio was assayed in control and SP-treated xenograft tumors (Table 1). Using HPLC as described, BH4 and BH2 levels were measured by acidic or alkaline oxidation to either biopterin or pterin. Untreated A549 tumors had a BH4:BH2 ratio of 3.92:1, while SP-treated tumors had a ratio of 6.10:1. This supports the previous finding that tumors, like other inflammatory conditions, exhibit low BH4:BH2 ratios that can be increased to more normal tissue levels using SP.

The coupling of NOS by SP and the production of NO can upregulate the cGMP/PKG pathway. This may subsequently lead to pro-apoptotic and anti-proliferative pathways. The results of the cGMP assay were inconclusive. One reason for this may be due to potentially high levels of phosphodiesterases (PDEs) that are expressed in tumor cells. My studies were not performed using PDE inhibitors.

	BH4:BH2
A549	3.92 ± 0.933
A549 + 1 mg/kg/ml SP	6.10 ± 0.69

Table 1. BH4:BH2 ratio. BH4:BH2 ratio was measured by HPLC in A549 flank tumor xenografts from untreated and SP-treated mice. N=5 for each group and data is reported as the mean +/- SEM.

SP increases the HbO_2 percentage in flank tumor xenografts.

Athymic nude mice were treated with 1 mg/kg/ml SP daily via drinking water for six days. The animals were imaged as described at three time points: prior to the first SP treatment, day 3 after the first SP treatment, and day 6 after the first SP treatment. MSOT data demonstrated that SP treatment increased the percentage of oxygenated hemoglobin in xenograft tumors when compared to control tumors (Figure 1). The percentage of oxygenated hemoglobin in the control tumors decreased over time. This was expected, since hypoxia increases as tumors grow. There is a significantly higher percentage of oxygenated hemoglobin in the SP-treated tumors versus control tumors after six days of SP treatment. The SP curve remains relatively constant – suggesting that the SP-treated tumors are not outgrowing their vasculature like the control tumors.

SP increases CD31 endothelial cell staining in A549 xenograft tumors.

Sections for CD31 staining were obtained from xenograft tumors from athymic nude mice treated with 1 mg/kg/ml SP via drinking water for two days. In the A549 xenograft model, CD31 staining was greater in tumors from mice treated with SP than in tumors from untreated mice (Figure 2). Staining was quantified by dividing the CD31 endothelial cell staining pixel intensity by the Hoechst nuclear staining pixel intensity. After only 2 days of SP treatment, there is a 26% increase in endothelial cell staining in SP-treated tumors compared to control tumors. This suggests that SP improves tumor vasculature in the xenograft tumors. Most of the staining is limited to the periphery of the tumors, a consequence of the xenograft tumor model.

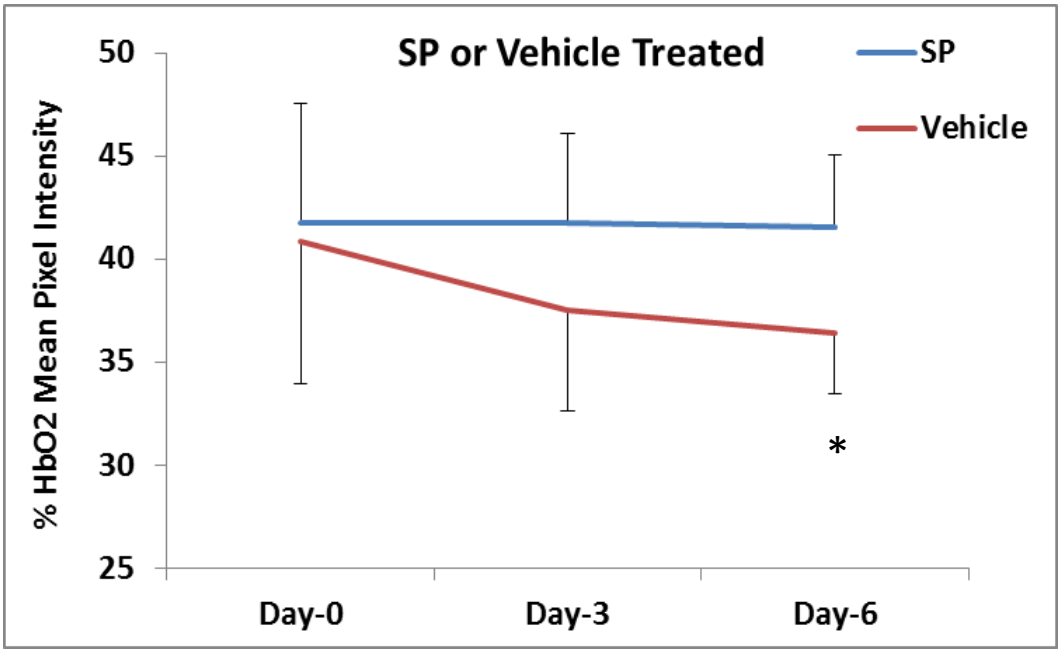

Figure 1. The effect of SP treatment on oxygenated hemoglobin levels in xenograft tumors. Mice were treated with 1 mg/kg/ml SP daily per mice via drinking water. The level of oxygenated hemoglobin decreased in vehicle treated mice, but remained steady in SP-treated mice. *$p<0.01$, n = 8 tumors.

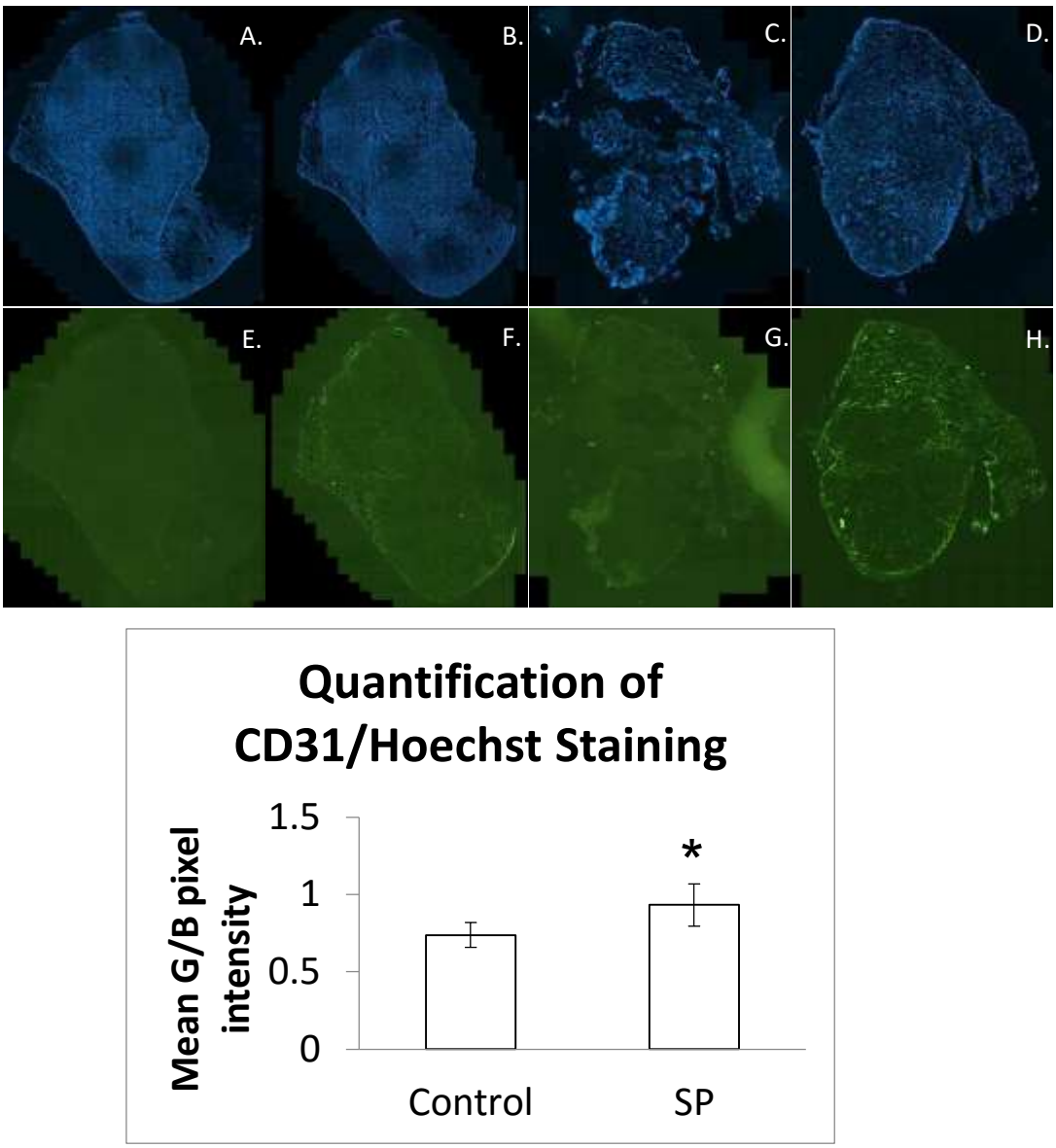

Figure 2. Increased CD31 staining in SP-treated A549 tumors.
Top: Images A - D are Hoechst stained A549 tumor sections with images E - H the corresponding CD31 stained sections with the blue Hoechst fluorescence turned off. Images A + E (no primary anti-CD31) and B + F (+ primary anti-CD31) are adjacent cryostat sections from the tumors of untreated animals; C + G (no primary anti-CD31) and D + H (+ primary anti-CD31) are adjacent cryostat sections from tumors of animals treated with SP.
Bottom: Quantification of staining. *$p < 0.05$, $n = 6$ tumors.

SP increases the percent of HbO_2 in MMTV spontaneous tumors.

Unlike the nude mice, the MMTV-neu mice were treated with SP by oral gavage in order to minimize variability from mouse to mouse. The mice were given 1 mg/kg/ml SP daily for six days. The animals were imaged as described at four time points: prior to the first SP treatment, day 5 after the first SP treatment, day 8 after the first SP treatment, and day 16 after the first SP treatment. MMTV tumors displayed an increased percentage of oxygenated hemoglobin, with a significant increase after eight days of SP treatment (Figure 3). There was also a decrease in hemoglobin oxygenation in control MMTV tumors. These results from the spontaneous tumor model provide additional evidence that SP treated tumors are not outgrowing their vasculature the way control tumors are, and are better oxygenated than untreated tumors.

SP decreases CD31 endothelial cell staining in MMTV spontaneous tumors.

Tumor sections for CD31 staining were obtained from the MMTV-neu mice used in MSOT imaging. After the mice were imaged on day 16, they were sacrificed. Tumors were subsequently extracted and stained as described. In the MMTV spontaneous tumor model, SP treatment resulted in less CD31 staining compared to control tumors (Figure 4). Spontaneous tumors displayed more staining in the central regions of the tumor than xenograft tumors, which have more peripheral staining.

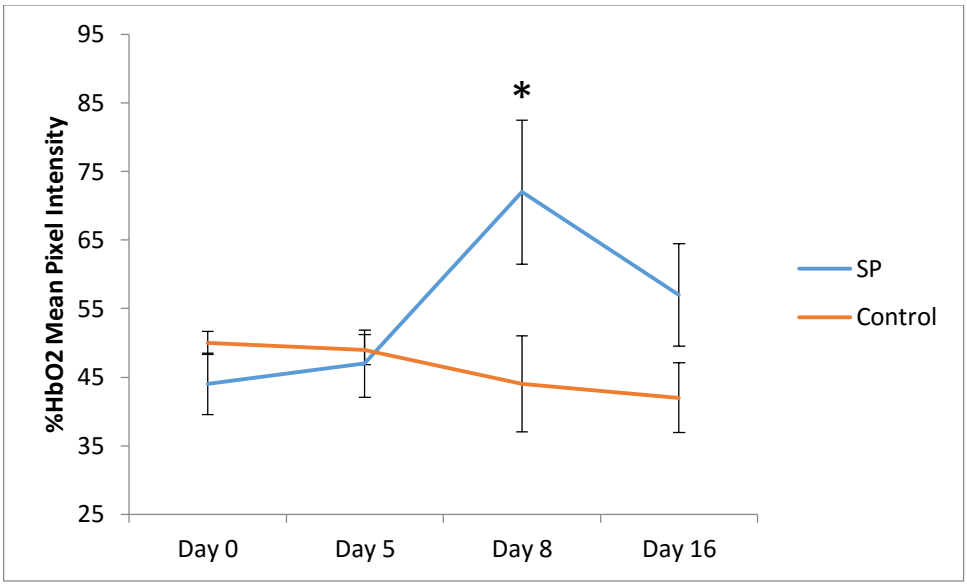

Figure 3. Effect of SP treatment on oxygenated hemoglobin levels in MMTV spontaneous tumors. Mice were treated with 1 mg/kg/ml SP daily per mouse by oral gavage. The level of oxygenated hemoglobin decreased in vehicle treated mice, but increased in SP-treated mice. *$p<0.05$, n = 7 tumors.

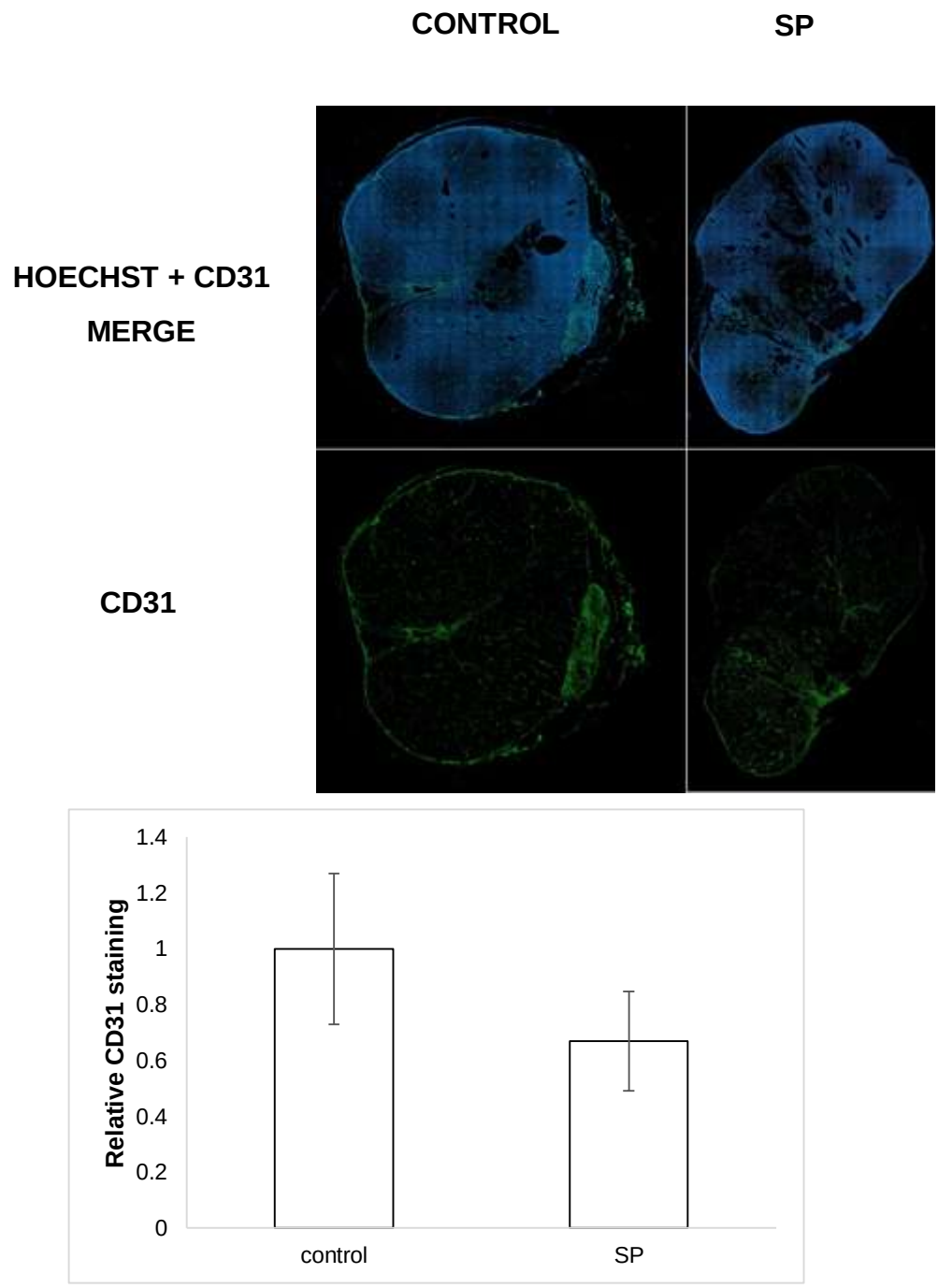

Figure 4. MMTV CD31 staining decreased with SP treatment. CD31 staining in MMTV tumors treated with SP was about 30% less than CD31 staining in control tumors. N=3 for each group.

Spontaneous tumors treated with SP have increased SMA staining.

SMA staining is useful for evaluating the relative pericyte content. Tumor sections for SMA staining were also obtained from the MMTV-neu mice used in MSOT imaging. After the mice were imaged on day 16, they were sacrificed. Tumors were subsequently extracted and stained as described. There is more than a two-fold increase in SMA staining 16 days post treatment (Figure 5). Increased SMA staining further suggests that the SP-treated tumors have a more improved vasculature than untreated control tumors.

Radiation response of xenograft tumors is variable in a cell survival assay.

Athymic nude mice with xenograft tumors were treated with 1 mg/kg/ml SP via drinking water for six days. The mice were then sacrificed and an ex vivo clonogenic assay was conducted as described. The survival of cells from mice that were both irradiated and treated with SP was variable (Figure 6). In the ex vivo clonogenic assay SP alone did not cause cell death. Irradiation, however, also did not cause significant death. This is because A549 cells do not show a significant radiation response at 2 Gy. The cell survival curve of A549 cells has a huge shoulder at 2 Gy, probably due to hypoxia. Panel B of Figure 6 splits the SP+IR bar to show the per cent survival for each tumor contributing to the SP+IR bar. The effects range from a 40% decrease to a 50% increase in cell survival. The variability observed may be due to variations among mice and their response to treatment.

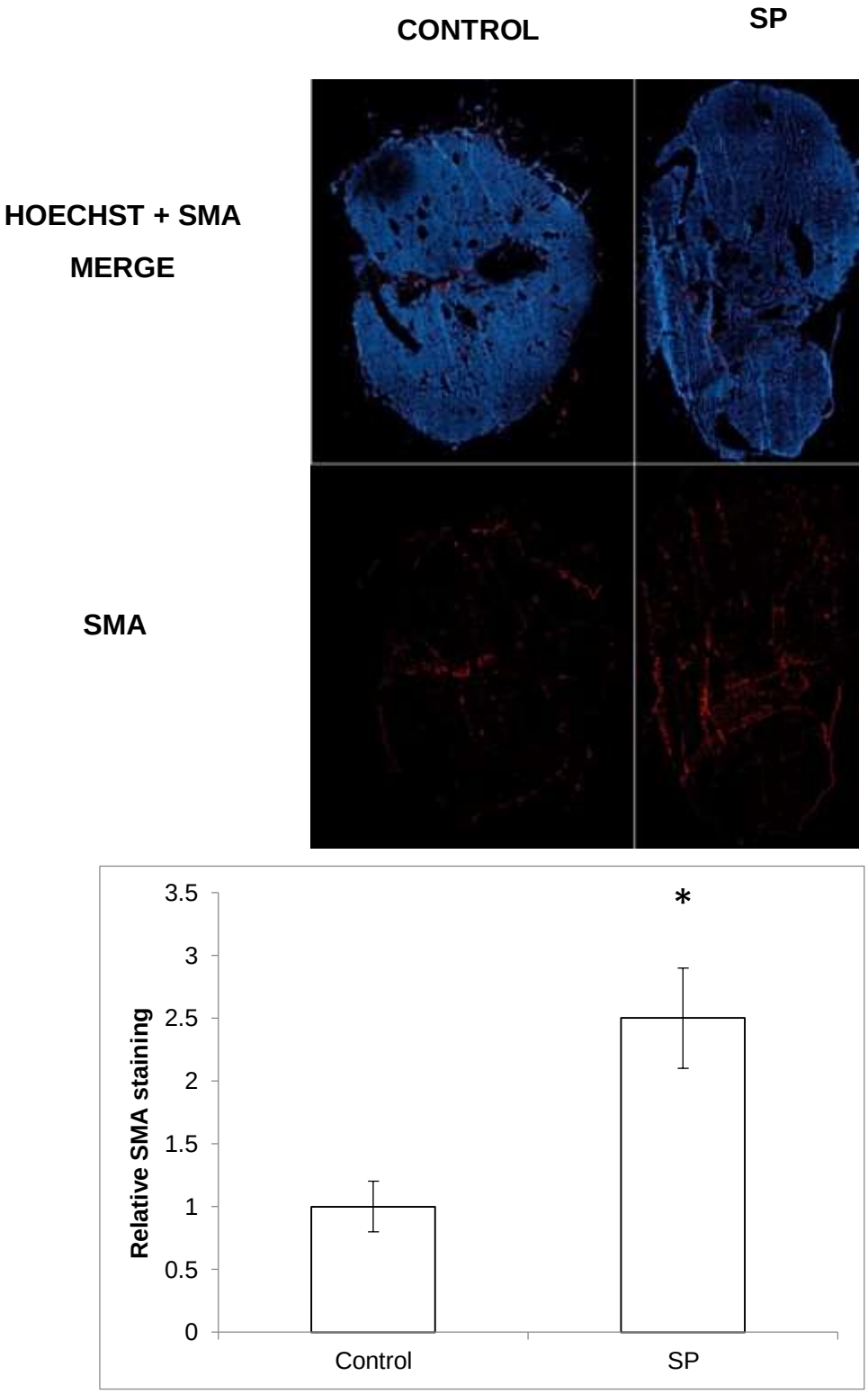

Figure 5. Quantification of SMA staining in MMTV tumors. Mice treated with 1mg/kg sepiapterin orally for 6 days had a more than two-fold increase in SMA staining at 16 days post the beginning of treatment. N=4 for each group. $p<.005$ by student's t test.

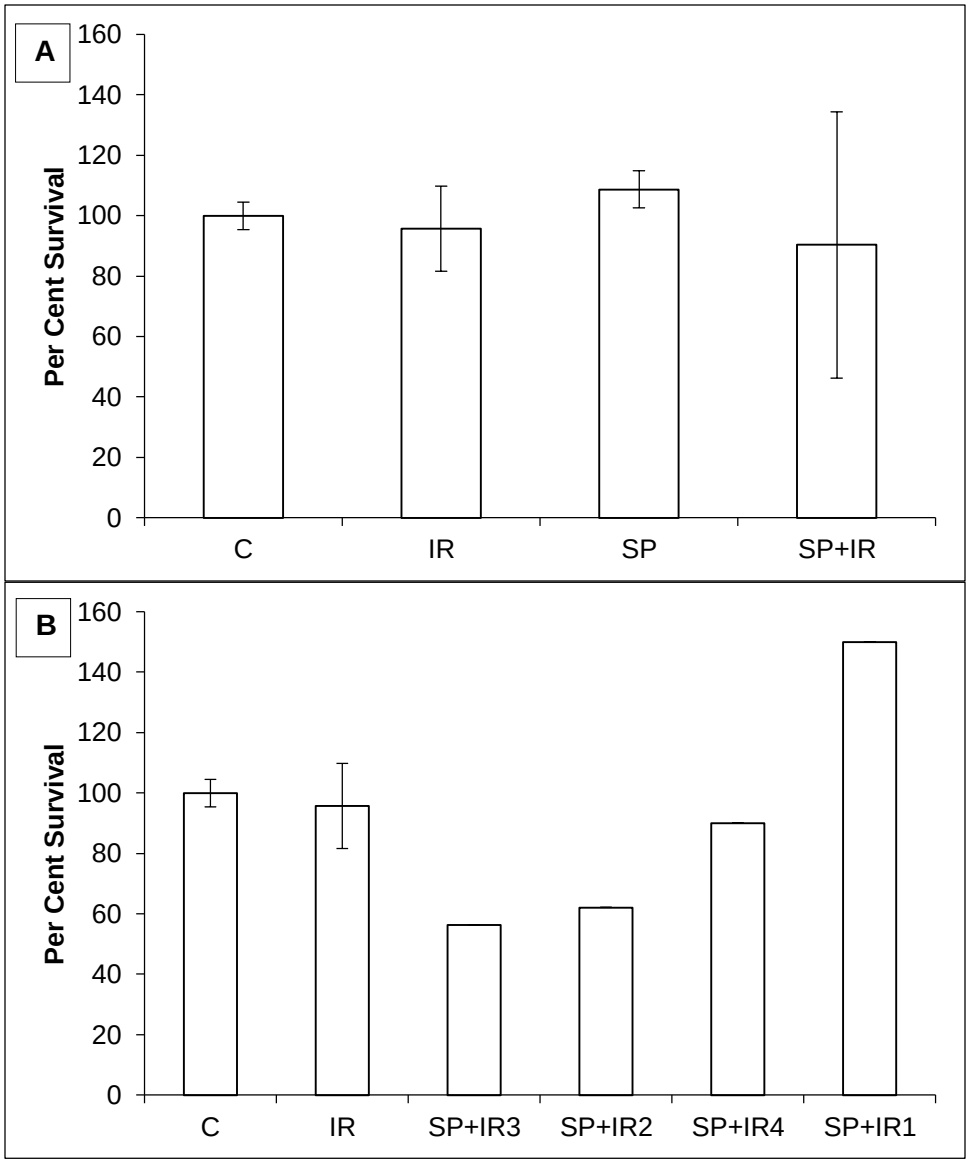

Figure 6. *In vivo* analysis of SP treatment and irradiation on A549 cell survival. Irradiated mice were treated at 2 Gy and SP-treated mice were given 1 mg/kg/ml SP daily via drinking water. Panel A illustrates the mean per cent survival for each of the four groups. A549 cells do not have a significant radiation response at 2 Gy, and the effect of SP treatment with IR is highly variable. Panel B illustrates the per cent survival of each SP plus IR treated tumor along with the mean survival for control and IR. The effect of SP with IR ranges from a 40% decrease in cell survival to a 50% increase in cell survival. Data is reported as the mean ± SD.

Xenograft tumors treated with SP and IR exhibit significant apoptosis.

Apoptosis was studied in xenograft tumors from mice treated with 1 mg/kg/ml SP daily for six days. Apoptag staining is used to visualize and identify apoptotic cells. The Apoptag kit was purchased from Millipore and staining was conducted as instructed in the manual. SP treatment of xenograft tumors with irradiation results in significantly more cell death than either vehicle or irradiation alone (Figure 7). This suggests that SP radiosensitizes A549 tumor cells.

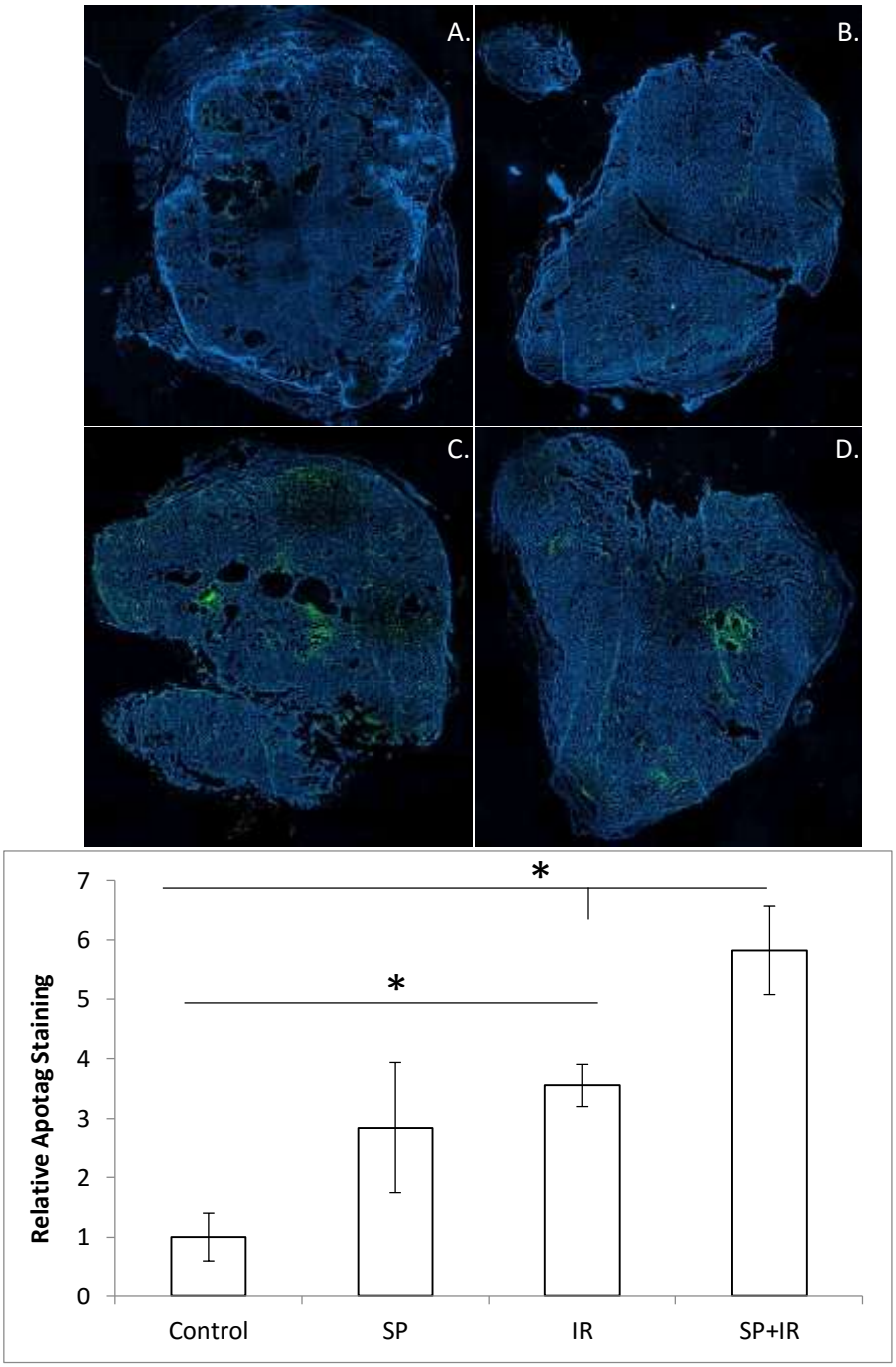

Figure 7. Apoptag staining in A549 xenografts.
1 mg/kg/ml SP given orally, once daily, significantly increases the level of apoptosis post 4Gy IR. A: untreated control,
B: SP-treated, C: IR alone, D: SP+IR. N=3 for each group.
* p<.01

DISCUSSION

SP treatment raised the BH4:BH2 ratio in A549 xenograft tumors and increased the percentage of oxygenated hemoglobin in both MMTV spontaneous and A549 xenograft tumor models. MMTV spontaneous tumors treated with SP exhibited less CD31 staining than untreated tumors, while A549 xenograft tumors had increased staining compared to control tumors. When SMA staining and hemoglobin oxygenation percentages are taken into account, these results do not appear so paradoxical. Xenograft models are more highly vascularized at the periphery of the tumors. Normalization in this model is likely to result in improved perfusion in more central regions of the tumor, resulting in more endothelial cell staining. In contrast, MMTV spontaneous tumors tend to be vascularized throughout the tumor, not simply the periphery. Normalization in this case may involve vascular reconstruction which may not necessarily involve a significant increase in endothelial cell expression but rather enhanced function especially with recruitment of vascular smooth muscle cells. The latter mechanism is supported by the SMA staining results in SP treated spontaneous tumors. Spontaneous tumor models also exhibit vasculature that is more typical of human tumors and thus are more useful in studies on the role of tumor vasculature in the response of tumors to chemotherapeutic drugs and radiation.

The precise mechanism by which SP normalizes tumor vasculature and improves oxygenation and perfusion was not investigated in this study. As stated before, angiogenesis and vascularization are complex processes that involve multiple pathways. However, our lab has previously demonstrated that SP reduces infiltration of

inflammatory macrophages and reduces inflammatory responses. Tumor associated macrophages are known to be important players in tumor progression. SP may influence the function of these macrophages in normalizing vasculature. Vessel normalization occurs during a transient window. Tumors exhibit a normalized vascular phenotype during this window of SP treatment, but the effects are lost after a few days. This is similar to what is observed with other agents that normalize tumor vasulature, such as avastin. In our studies the greatest effect on cell death, CD31 staining, and SMA staining was observed at 8 days.

Irradiation following SP treatment produced variable results in tumors when analyzed by an ex-vivo clonogenic assay, but Apoptag analysis indicated significant apoptosis in SP-treated tumors compared to tumors from mice that were only irradiated. The variability in the clonogenic assay may be attributed to the method of SP delivery; mice were treated with SP via drinking water. The mice may have ingested varying amounts of SP depending on how much water was consumed by each mouse each day. The significant apoptosis visualized in Apoptag analysis suggests SP treatment reinforces the effects of radiation and induces radiosensitization.

Besides vascular remodeling, there may be other underlying molecular pathways that help confer radiosensitivity upon tumors. Our lab has previously demonstrated that SP has significant effects on downstream signaling. SP upregulates cGMP-dependent PKG activity, reduces NF-κB promotor activity, and downregulates β-catenin and TCF4 promoter activity [49]. To study the potential involvement of molecular pathways in SP treatment independent of vascular changes, tumor cells were studied *in vitro*. An *in vitro* clonogenic assay was conducted using A549 tumor cells. Cells were treated with

sepiapterin 24, 48, or 72 hours prior to 2 Gy irradiation. The SP-containing media was removed and replaced with fresh media 24 hours prior to irradiation in all dishes except for the dishes that were treated with SP 24 hours prior to irradiation. SP was not kept on board during irradiation because it has previously been shown to be radioprotective when kept on board. SP significantly decreased cell survival in cells treated 48 hours prior to irradiation compared to cells that were irradiated alone (Figure 8). This indicates that SP also works directly on epithelial cells, since *in vitro* models lack vasculature.

One potential mechanism may involve STAT3, which is involved in pro-survival pathways, and the overexpression of which has been observed in numerous cancers [50, 5]. Oxygenation has been shown to downregulate expression of STAT3 and cyclin-D1, inhibiting tumor growth in ovarian cancer [51]. Inhibition of STAT3 has also been shown to reverse radioresistance in human lung cancer [52]. SP potentially downregulates STAT3 post radiation therapy. Our lab has previously shown that STAT3 is phosphorylated following irradiation in the A549 cells. This cell line in particular is known to exhibit radioresistance. SP may potentially downregulate STAT3 post-radiation to radiosensitize tumor cells.

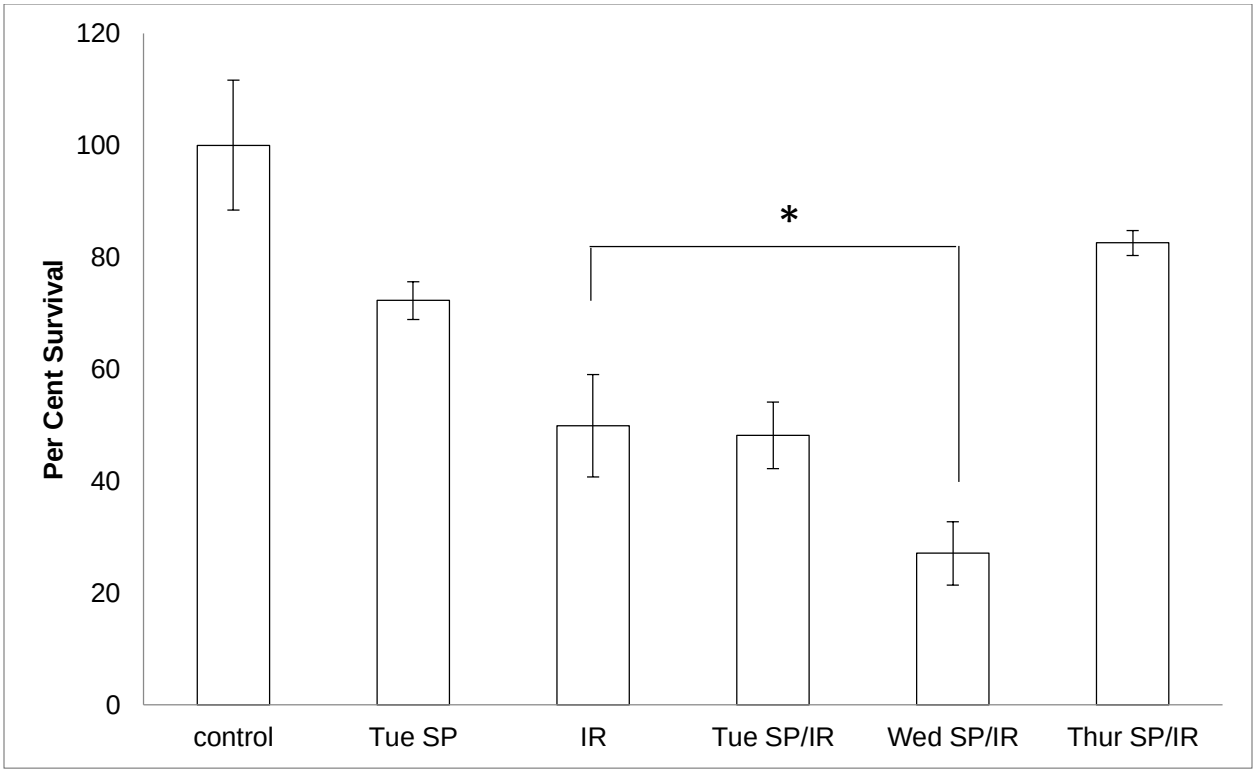

Figure 8. *In vitro* analysis of SP and irradiation cell survival. Dishes were treated with 20 µM SP. Tue SP/IR dishes were treated with SP 24 hours prior to irradiation. Wed SP/IR dishes were treated with SP 48 hours prior to irradiation. Thur SP/IR dishes were treated with SP 72 hours prior to irradiation. Treatment of cells with SP 48 hours prior to irradiation significantly decreased cell survival. Data is reported as the mean ± SD. * $p<0.05$ by student's t-test, n=3 for each group.

Sepiapterin normalizes tumor vasculature, radiosensitizes tumors, and oxygenates tumors. This suggests that the increased perfusion will also improve delivery of vital therapeutic drugs. Sepiapterin is already used in the treatment of some forms of phenylketonuria. For a number of vascular diseases, SP is also in clinical trials for treatment of endothelial dysfunction. SP is potentially a safe alternative to other normalizing agents, such as avastin, which are associated with considerable toxicity [53]. In addition to low toxicity, SP demonstrates anti-proliferative properties in MMTV and other breast tumor models, alleviating concerns that it may be pro-tumorigenic [54]. In future studies, the efficiency of drugs like doxorubicin may be studied following SP treatment to investigate how SP will affect drug delivery. Radioresistance and inefficient drug delivery hinder cancer treatment, but SP appears promising in combating these obstacles to therapy.

References

1. Jain, Rakesh K. “Normalizing Tumor Microenvironment to Treat Cancer: Bench to Bedside to Biomarkers.” *Journal of Clinical Oncology* 31, no. 17 (June 10, 2013): 2205–18. doi:10.1200/JCO.2012.46.3653.
2. Nagy, J. A., S.-H. Chang, A. M. Dvorak, and H. F. Dvorak. “Why Are Tumour Blood Vessels Abnormal and Why Is It Important to Know?” *British Journal of Cancer* 100, no. 6 (February 24, 2009): 865–69. doi:10.1038/sj.bjc.6604929.
3. Vaupel, Peter, Friedrich Kallinowski, and Paul Okunieff. “Blood Flow, Oxygen and Nutrient Supply, and Metabolic Microenvironment of Human Tumors: A Review.” *Cancer Research* 49, no. 23 (December 1, 1989): 6449–65.
4. Al-Husein, Belal, Maha Abdalla, Morgan Trepte, David L. DeRemer, and Payaningal R. Somanath. “Anti-Angiogenic Therapy for Cancer: An Update.” *Pharmacotherapy* 32, no. 12 (December 2012): 1095–1111. doi:10.1002/phar.1147.
5. Vara, Juan Ángel Fresno, Enrique Casado, Javier de Castro, Paloma Cejas, Cristóbal Belda-Iniesta, and Manuel González-Barón. “PI3K/Akt Signalling Pathway and Cancer.” *Cancer Treatment Reviews* 30, no. 2 (April 2004): 193–204. doi:10.1016/j.ctrv.2003.07.007.
6. Ribatti, Domenico, Angelo Vacca, and Franco Dammacco. “The Role of the Vascular Phase in Solid Tumor Growth: A Historical Review.” *Neoplasia (New York, N.Y.)* 1, no. 4 (October 1999): 293–302.
7. Byrne, Annette T., Leorah Ross, Joceyln Holash, Mikiye Nakanishi, Limin Hu, Judith I. Hofmann, George D. Yancopoulos, and Robert B. Jaffe. “Vascular Endothelial Growth Factor-Trap Decreases Tumor Burden, Inhibits Ascites, and Causes Dramatic Vascular Remodeling in an Ovarian Cancer Model.” *Clinical Cancer Research* 9, no. 15 (November 15, 2003): 5721–28.
8. Bergers, Gabriele, and Laura E. Benjamin. “Tumorigenesis and the Angiogenic Switch.” *Nature Reviews Cancer* 3, no. 6 (June 2003): 401–10. doi:10.1038/nrc1093.
9. Ivy, S. Percy, Jeannette Y. Wick, and Bennett M. Kaufman. “An Overview of Small-Molecule Inhibitors of VEGFR Signaling.” *Nature Reviews Clinical Oncology* 6, no. 10 (October 2009): 569–79. doi:10.1038/nrclinonc.2009.130.
10. “Endothelial Receptor Tyrosine Kinases Activate the STAT Signaling Pathway: Mutant Tie-2 Causing Venous Malformations Signals a Distinct STAT Activation Response.” *, Published Online: 19 January 1999; | doi:10.1038/sj.onc.1202288* 18, no. 1 (January 19, 1999). doi:10.1038/sj.onc.1202288.
11. Goel, Hira Lal, and Arthur M. Mercurio. “VEGF Targets the Tumour Cell.” *Nature Reviews Cancer* 13, no. 12 (December 2013): 871–82. doi:10.1038/nrc3627.
12. Abedi, Husna, and Ian Zachary. “Vascular Endothelial Growth Factor Stimulates Tyrosine Phosphorylation and Recruitment to New Focal Adhesions of Focal Adhesion Kinase and Paxillin in Endothelial Cells.” *Journal of Biological Chemistry* 272, no. 24 (June 13, 1997): 15442–51. doi:10.1074/jbc.272.24.15442.
13. Le, Ngoc Hang, Paola van der Bent, Gerwin Huls, Marc van de Wetering, Mahmoud Loghman-Adham, Albert C. M. Ong, James P. Calvet, et al. “Aberrant

Polycystin-1 Expression Results in Modification of Activator Protein-1 Activity, Whereas Wnt Signaling Remains Unaffected." *Journal of Biological Chemistry* 279, no. 26 (June 25, 2004): 27472–81. doi:10.1074/jbc.M312183200.
14. Hermann, Corinna, Birgit Assmus, Carmen Urbich, Andreas M. Zeiher, and Stefanie Dimmeler. "Insulin-Mediated Stimulation of Protein Kinase Akt A Potent Survival Signaling Cascade for Endothelial Cells." *Arteriosclerosis, Thrombosis, and Vascular Biology* 20, no. 2 (February 1, 2000): 402–9. doi:10.1161/01.ATV.20.2.402.
15. Fujio, Yasushi, and Kenneth Walsh. "Akt Mediates Cytoprotection of Endothelial Cells by Vascular Endothelial Growth Factor in an Anchorage-Dependent Manner." *Journal of Biological Chemistry* 274, no. 23 (June 4, 1999): 16349–54. doi:10.1074/jbc.274.23.16349.
16. Guo, Chunqing, Annicole Buranych, Devanand Sarkar, Paul B. Fisher, and Xiang-Yang Wang. "The Role of Tumor-Associated Macrophages in Tumor Vascularization." *Vascular Cell* 5, no. 1 (2013): 20. doi:10.1186/2045-824X-5-20.
17. Raza, Ahmad, Michael J. Franklin, and Arkadiusz Z. Dudek. "Pericytes and Vessel Maturation during Tumor Angiogenesis and Metastasis." *American Journal of Hematology* 85, no. 8 (August 1, 2010): 593–98. doi:10.1002/ajh.21745.
18. Hvingel, Bodil, Marit Lieng, Borghild Roald, and Anne Ørbo. "Vascular Markers CD31, CD34, Actin, VEGFB, and VEGFR2, Are Prognostic Markers for Malignant Development in Benign Endometrial Polyps." *Open Journal of Obstetrics and Gynecology* 02, no. 01 (2012): 18–26. doi:10.4236/ojog.2012.21004.
19. Tonino, Paola, and Carmen Abreu. "Microvessel Density Is Associated with VEGF and α-SMA Expression in Different Regions of Human Gastrointestinal Carcinomas." *Cancers* 3, no. 3 (2011): 3405–18. doi:10.3390/cancers3033405.
20. Xu, Weiming, Li Zhi Liu, Marilena Loizidou, Mohamed Ahmed, and Ian G. Charles. "The Role of Nitric Oxide in Cancer." *Cell Research* 12, no. 5 (2002): 311–20. doi:10.1038/sj.cr.7290133.
21. Shen, WEIQUN, XIAOPING Zhang, GONG Zhao, MICHAEL S. Wolin, WILLIAM Sessa, and THOMAS H. Hintze. "Nitric Oxide Production and NO Synthase Gene Expression Contribute to Vascular Regulation during Exercise." *Medicine & Science in Sports & Exercise* 27, no. 8 (August 1995): 1125–34.
22. Nathan, Carl, and Qiao-wen Xie. "Nitric Oxide Synthases: Roles, Tolls, and Controls." *Cell* 78, no. 6 (September 23, 1994): 915–18. doi:10.1016/0092-8674(94)90266-6.
23. Fukumura, Dai, Satoshi Kashiwagi, and Rakesh K. Jain. "The Role of Nitric Oxide in Tumour Progression." *Nature Reviews Cancer* 6, no. 7 (July 2006): 521–34. doi:10.1038/nrc1910.
24. Friebe, Andreas, and Doris Koesling. "Regulation of Nitric Oxide-Sensitive Guanylyl Cyclase." *Circulation Research* 93, no. 2 (July 25, 2003): 96–105. doi:10.1161/01.RES.0000082524.34487.31.
25. Friebe, Andreas, and Doris Koesling. "Regulation of Nitric Oxide-Sensitive Guanylyl Cyclase." *Circulation Research* 93, no. 2 (July 25, 2003): 96–105. doi:10.1161/01.RES.0000082524.34487.31.

26. Parmentier, S., G. A. Böhme, D. Lerouet, D. Damour, J. M. Stutzmann, I. Margaill, and M. Plotkine. “Selective Inhibition of Inducible Nitric Oxide Synthase Prevents Ischaemic Brain Injury.” *British Journal of Pharmacology* 127, no. 2 (May 1999): 546–52. doi:10.1038/sj.bjp.0702549.
27. Dean, Michael, Tito Fojo, and Susan Bates. “Tumour Stem Cells and Drug Resistance.” *Nature Reviews Cancer* 5, no. 4 (April 2005): 275–84. doi:10.1038/nrc1590.
28. Kostourou, V, S P Robinson, J E Cartwright, and G St J Whitley. “Dimethylarginine Dimethylaminohydrolase I Enhances Tumour Growth and Angiogenesis.” *British Journal of Cancer* 87, no. 6 (September 9, 2002): 673–80. doi:10.1038/sj.bjc.6600518.
29. Kashiwagi, Satoshi, Kosuke Tsukada, Lei Xu, Junichi Miyazaki, Sergey V. Kozin, James A. Tyrrell, William C. Sessa, Leo E. Gerweck, Rakesh K. Jain, and Dai Fukumura. “Perivascular Nitric Oxide Gradients Normalize Tumor Vasculature.” *Nature Medicine* 14, no. 3 (March 2008): 255–57. doi:10.1038/nm1730.
30. Jain, Rakesh K. “Normalizing Tumor Vasculature with Anti-Angiogenic Therapy: A New Paradigm for Combination Therapy.” *Nature Medicine* 7, no. 9 (September 2001): 987–89. doi:10.1038/nm0901-987.
31. Bergers, Gabriele, and Douglas Hanahan. “Modes of Resistance to Anti-Angiogenic Therapy.” *Nature Reviews Cancer* 8, no. 8 (August 2008): 592–603. doi:10.1038/nrc2442.
32. Huang, Dongsheng, Huanrong Lan, Fanlong Liu, Shibing Wang, Xiaoyi Chen, Ketao Jin, and Xiaozhou Mou. “Anti-Angiogenesis or pro-Angiogenesis for Cancer Treatment: Focus on Drug Distribution.” *International Journal of Clinical and Experimental Medicine* 8, no. 6 (June 15, 2015): 8369–76.
33. Wong, Ping-Pui, Fevzi Demircioglu, Essam Ghazaly, Wasfi Alrawashdeh, Michael R. L. Stratford, Cheryl L. Scudamore, Biancastella Cereser, et al. “Dual-Action Combination Therapy Enhances Angiogenesis While Reducing Tumor Growth and Spread.” *Cancer Cell* 27, no. 1 (January 12, 2015): 123–37. doi:10.1016/j.ccell.2014.10.015.
34. Nguyen, Giang Huong, Mandi M. Murph, and Joe Y. Chang. “Cancer Stem Cell Radioresistance and Enrichment: Where Frontline Radiation Therapy May Fail in Lung and Esophageal Cancers.” *Cancers* 3, no. 1 (March 10, 2011): 1232–52. doi:10.3390/cancers3011232.
35. Tim Tak Kwok, and Robert M. Sutherland. “The Eighth International Conference on Chemical Modifiers of Cancer Treatment Repair of Potentially Lethal Radiation Damage in Human Squamous Carcinoma Cells after Chronic Hypoxia.” *International Journal of Radiation Oncology*Biology*Physics* 29, no. 2 (May 15, 1994): 255–58. doi:10.1016/0360-3016(94)90271-2.
36. Carlson, David J., Kamil M. Yenice, and Colin G. Orton. “Tumor Hypoxia Is an Important Mechanism of Radioresistance in Hypofractionated Radiotherapy and Must Be Considered in the Treatment Planning Process.” *Medical Physics* 38, no. 12 (December 1, 2011): 6347–50. doi:10.1118/1.3639137.
37. Kim, John J., and Ian F. Tannock. “Repopulation of Cancer Cells during Therapy: An Important Cause of Treatment Failure.” *Nature Reviews Cancer* 5, no. 7 (July 2005): 516–25. doi:10.1038/nrc1650.

38. Pajonk, Frank, Erina Vlashi, and William H. McBride. “Radiation Resistance of Cancer Stem Cells: The 4 R’s of Radiobiology Revisited.” *Stem Cells (Dayton, Ohio)* 28, no. 4 (April 2010): 639–48. doi:10.1002/stem.318.
39. Huang, Qian, Fang Li, Xinjian Liu, Wenrong Li, Wei Shi, Fei-Fei Liu, Brian O’Sullivan, et al. “Caspase 3-Mediated Stimulation of Tumor Cell Repopulation during Cancer Radiotherapy.” *Nature Medicine* 17, no. 7 (July 3, 2011): 860–66. doi:10.1038/nm.2385.
40. Dean, Michael, Tito Fojo, and Susan Bates. “Tumour Stem Cells and Drug Resistance.” *Nature Reviews Cancer* 5, no. 4 (April 2005): 275–84. doi:10.1038/nrc1590.
41. Bonavida, Benjamin, and Stavroula Baritaki. “Inhibition of Epithelial-to-Mesenchymal Transition (EMT) in Cancer by Nitric Oxide: Pivotal Roles of Nitrosylation of NF-κB, YY1 and Snail.” *Forum on Immunopathological Diseases and Therapeutics* 3, no. 2 (2012): 125–33. doi:10.1615/ForumImmunDisTher.2012006065.
42. Baritaki, Stavroula, Sara Huerta-Yepez, Anna Sahakyan, Iordanis Karagiannides, Kyriaki Bakirtzi, Ali R Jazirehi, and Benjamin Bonavida. “Mechanisms of Nitric Oxide-Mediated Inhibition of EMT in Cancer.” *Cell Cycle* 9, no. 24 (December 15, 2010): 4931–40. doi:10.4161/cc.9.24.14229.
43. Gao, Xiaohuan, Debabrata Saha, Payal Kapur, Thomas Anthony, Edward H. Livingston, and Sergio Huerta. “Radiosensitization of HT-29 Cells and Xenografts by the Nitric Oxide Donor DETANONOate.” *Journal of Surgical Oncology* 100, no. 2 (August 1, 2009): 149–58. doi:10.1002/jso.21318.
44. Morton, Christopher L., and Peter J. Houghton. “Establishment of Human Tumor Xenografts in Immunodeficient Mice.” *Nature Protocols* 2, no. 2 (February 2007): 247–50. doi:10.1038/nprot.2007.25.
45. Janssens, Marleen Y., Dirk L. Van den Berge, Valeri N. Verovski, Christinne Monsaert, and Guy A. Storme. “Activation of Inducible Nitric Oxide Synthase Results in Nitric Oxide-Mediated Radiosensitization of Hypoxic EMT-6 Tumor Cells.” *Cancer Research* 58, no. 24 (December 15, 1998): 5646–48.
46. Ellinsworth, David C. “Arsenic, Reactive Oxygen, and Endothelial Dysfunction.” *Journal of Pharmacology and Experimental Therapeutics* 353, no. 3 (June 1, 2015): 458–64. doi:10.1124/jpet.115.223289.
47. Xu, Weiming, Li Zhi Liu, Marilena Loizidou, Mohamed Ahmed, and Ian G. Charles. “The Role of Nitric Oxide in Cancer.” *Cell Research* 12, no. 5 (2002): 311–20. doi:10.1038/sj.cr.7290133.
48. Rabender, Christopher S., Asim Alam, Gobalakrishnan Sundaresan, Robert J. Cardnell, Vasily A. Yakovlev, Nitai D. Mukhopadhyay, Paul Graves, Jamal Zweit, and Ross B. Mikkelsen. “The Role of Nitric Oxide Synthase Uncoupling in Tumor Progression.” *Molecular Cancer Research* 13, no. 6 (June 1, 2015): 1034–43. doi:10.1158/1541-7786.MCR-15-0057-T.
49. Windham, Perrin F., and Heather N. Tinsley. “cGMP Signaling as a Target for the Prevention and Treatment of Breast Cancer.” *Seminars in Cancer Biology*, Intracellular Signaling and Response to Anti-Cancer Therapy, 31 (April 2015): 106–10. doi:10.1016/j.semcancer.2014.06.006.

50. Bournazou, Eirini, and Jacqueline Bromberg. “Targeting the Tumor Microenvironment.” *JAK-SAT* 2, no. 2 (April 1, 2013): e23828. doi:10.4161/jkst.23828.
51. Selvendiran, Karuppaiyah, M. Lakshmi Kuppusamy, Shabnam Ahmed, Anna Bratasz, Guruguhan Meenakshisundaram, Brian K. Rivera, Mahmood Khan, and Periannan Kuppusamy. “Oxygenation Inhibits Ovarian Tumor Growth by Downregulating STAT3 and Cyclin-D1 Expressions.” *Cancer Biology & Therapy* 10, no. 4 (August 15, 2010): 386–90.
52. You, Shuo, Rui Li, Dongkyoo Park, Maohua Xie, Gabriel L. Sica, Ya Cao, Zhi-Qiang Xiao, and Xingming Deng. “Disruption of STAT3 by Niclosamide Reverses Radioresistance of Human Lung Cancer.” *Molecular Cancer Therapeutics* 13, no. 3 (March 2014): 606–16. doi:10.1158/1535-7163.MCT-13-0608.
53. Carroll, N. M. et. al. “Use of Bevacizumab in Community Settings: Toxicity Profile With Advanced Non-Small Cell Lung Cancer.” *Journal of Oncology Practice* 11, no. 5 (September 2015):356-362.
54. Burton BK, et al. Safety of extended treatment with sapopterin dihydrochloride in patients with phenylketonuria: results of a phase 3b study. *Mol. Genet. Metab.* 2011;103(4):315-22.